Journal of Biomolecular NMR **29:** 369–376, 2004.

$^{1}H,^{13}C$-$^{1}H,^{1}H$ dipolar cross-correlated spin relaxation in methyl groups

Vitali Tugarinov & Lewis E. Kay
Protein Engineering Network Centres of Excellence and the Departments of Medical Genetics, Biochemistry and Chemistry, University of Toronto, Toronto, Ontario, Canada M5S 1A8

Received 12 January 2004; Accepted 27 February 2004

Key words: cross-correlated dipolar spin relaxation, methyl groups, order parameter

Abstract

Relaxation in methyl groups is strongly influenced by cross-correlated interactions involving the methyl dipoles. One of the major interference effects results from intra-methyl ^{1}H-^{13}C, ^{1}H-^{1}H dipolar interactions, leading to significant differences in the relaxation of certain multiplet components that contribute to double- and zero-quantum ^{1}H-^{13}C spectra. NMR experiments are presented for the measurement of this differential relaxation effect. It is shown that this difference in relaxation between double- and zero-quantum multiplet components can be used as a sensitive reporter of side chain dynamics and that accurate methyl axis order parameters can be measured in proteins that tumble with correlation times greater than approximately 5 ns.

Introduction

Over the past several decades a significant number of papers have appeared describing experimental and theoretical studies of the spin dynamics of methyl groups (Kay et al., 1992a; Kay and Prestegard, 1987; Kay and Torchia, 1991; Muller et al., 1987; Palmer et al., 1991; Werbelow and Grant, 1977; Werbelow and Marshall, 1973). The complexity of the underlying spin physics becomes readily apparent when one considers the fact that for an isolated $^{13}CH_3$ group there are 10 single-quantum ^{1}H transitions, a further 8 ^{13}C transitions, as well as a large number of various multiple-quantum transitions. These transitions are, in turn, relaxed via a complex network of dipolar and chemical shift anisotropy interactions that give rise to differential relaxation effects (Kay and Bull, 1992; Vold and Vold, 1976; Werbelow and Marshall, 1973). Such effects must be considered in any analysis of methyl ^{13}C or ^{1}H relaxation as a probe of molecular dynamics (Kay et al., 1992a), or in the case where intensities of methyl correlations in spectra are to be understood quantitatively (Tugarinov et al., 2003).

Despite the inherent complexities that cross-correlated spin relaxation adds to the above analyses, it can be put to good use. Werbelow and Grant (1977), among others (Prestegard and Grant, 1978; Vold and Vold, 1978), have exploited such effects to obtain detailed information about dynamics of molecules. More recently, our laboratory has shown that relaxation interference effects involving intra-methyl ^{1}H-^{1}H and ^{1}H-^{13}C dipolar interactions can be exploited in recording ^{1}H-^{13}C HMQC spectra of methyl groups in high molecular weight proteins that are of significantly higher sensitivity and resolution than the corresponding correlation spectra obtained using the much more common HSQC scheme (Ollerenshaw et al., 2003; Tugarinov et al., 2003). The enhancements can be explained in terms of a dipolar TROSY effect that is magnetic field independent and that depends critically on cross-correlated spin relaxation.

Our goal here is to further investigate the rich network of relaxation interactions that manifest in a $^{13}CH_3$ spin system. Specifically, we focus on ^{1}H-^{13}C multiple-quantum (MQ) transitions that are of importance in HMQC spectroscopy and study the difference between the relaxation of the DQ (double-quantum) and ZQ (zero-quantum) elements that comprise this MQ coherence. As described previously, many of the relaxation interactions that are of relevance for these MQ transitions are extremely efficient and they scale with molecular weight (Ollerenshaw et al., 2003;

Tugarinov et al., 2003). We have, therefore, chosen to focus on a small 7.5 kDa protein, protein L (τ_C = 5.0 ns at 25 °C, D_2O). Multiplet components that would normally disappear or be very small in applications to large proteins are now visible and relaxation interactions can be quantified. We show that the relaxation rates of certain multiplet components depend very significantly on intra-methyl ^1H-^{13}C/^1H-^1H dipolar cross-correlation effects and that these rates can, in many cases, be used to obtain accurate estimates of the amplitudes of motion of the methyl symmetry axis.

Materials and methods

NMR sample preparation

A U-[^{15}N,^2H], Ileδ1-[$^{13}CH_3$], Leu,Val-[$^{13}CH_3$/$^{12}CD_3$]-labeled sample of the B1 immunoglobulin binding domain of peptostreptoccocal protein L (Scalley et al., 1997) was obtained by protein overexpression from a culture of *E. coli* BL21(DE3) cells in 1 l D_2O M9 media using U-[^2H]-glucose and $^{15}NH_4Cl$ (CIL, Andover, MA) as the carbon and nitrogen sources, respectively (Tugarinov and Kay, 2004). The addition of 80 mg of 2-keto-3,3-d_2-4-^{13}C-butyrate and 120 mg of 2-keto-3-methyl-d_3-3-d_1-4-^{13}C-butyrate (α-ketoisovalerate deuterated at the β-position with one of the two methyl groups – $^{12}CD_3$) to the growth medium one hour prior to induction led to the production of a highly deuterated protein with protonation restricted to Ile δ1 methyls and one of the methyl groups of Leu and Val residues (Leu,Val-[$^{13}CH_3$,$^{12}CD_3$]). The sodium salts of 2-keto-4-^{13}C-butyric and 2-keto-3-methyl-d_3-4-^{13}C-butyric acids were obtained from Isotec (Miamisburg, OH), and the 3-[^1H] positions subsequently exchanged to ^2H according to Gardner and Kay (1997) and Goto et al. (1999) Details of protein expression and purification have been described previously (Mittermaier and Kay, 2001). The NMR sample contained 99.9% D_2O, 50 mM sodium phosphate buffer (pH 6.0, uncorrected) and was 1.4 mM in protein.

NMR spectroscopy

NMR experiments were performed on a 600 MHz Varian Inova spectrometer equipped with a pulsed-field gradient triple resonance probe. Relaxation rates of the outer multiplet components of correlations in ^1H-^{13}C double-quantum (DQ) and zero-quantum (ZQ) spectra (pulse sequence of Figure 2a) were obtained from data sets recorded with acquisition times of (60 ms, 64 ms) in the (^{13}C,^1H) dimensions and parametrically varied delays T of 2, 6, 10, 14, 18, 22, 26, 30, 34, 38 ms (5 °C, 15 °C) and 10, 18, 26, 34, 42, 50, 58, 66, 74, 82 ms (25 °C). Delays T = 1, 14, 30, 47, 67, 90, 116, 150 ms (5 °C), T = 1, 8, 24, 40, 72, 104, 136, 168 ms (15 °C), and T = 4, 16, 32, 48, 68, 88, 116, 152 ms (25 °C) were used in measurements of relaxation rates of the central multiplet component of correlations in DQ and ZQ spectra (scheme of Figure 2b). A relaxation delay of 1.0 sec and 16(8) scans/fid were used, resulting in net acquisition times of ∼50(25) min/spectrum for the measurements involving the outer(central) multiplet components.

The molecular tumbling correlation times (τ_c, assumed isotropic) of protein L (D_2O) were obtained from ^{15}N relaxation measurements performed on samples dissolved in H_2O, subsequently scaled by the ratio of viscosities of D_2O to H_2O at a given temperature, ν^T_{D2O}/ν^T_{H2O}. Ratios of translational diffusion constants obtained from measurements on protein L samples in H_2O and D_2O at 5 °C and 25 °C are in quantitative agreement with tabulated ratios of viscosities for H_2O and D_2O (Cho et al., 1999), suggesting that the method of scaling the protein correlation times measured in H_2O to those in D_2O is appropriate. All NMR spectra were processed using programs from NMRPipe/NMRDraw (Delaglio et al., 1995) and analyzed using Matlab v.6 software (MathWorks, Inc., MA).

Results and discussion

Prior to a description of our studies on protein L it is worthwhile to briefly review some of the essential features pertaining to the magnetization flow in a $^{13}CH_3$ spin system during the course of a simple HMQC pulse scheme. The net transfer of magnetization is given by $^1H \rightarrow {}^1H$-^{13}C MQ (t_1)$\rightarrow {}^1H$ (t_2), but this simple scheme, unfortunately, provides no insight into what is happening at the level of individual coherences, which behave quite differently during the pulse sequence (Tugarinov et al., 2003). A more detailed analysis that has been presented elsewhere (Ollerenshaw et al., 2003; Tugarinov et al., 2003), shows that in the macromolecular limit and assuming rapid methyl rotation, there are both fast and slowly relaxing ^1H SQ and ^1H-^{13}C MQ transitions and that, for an isolated methyl group, the transfer pathways do

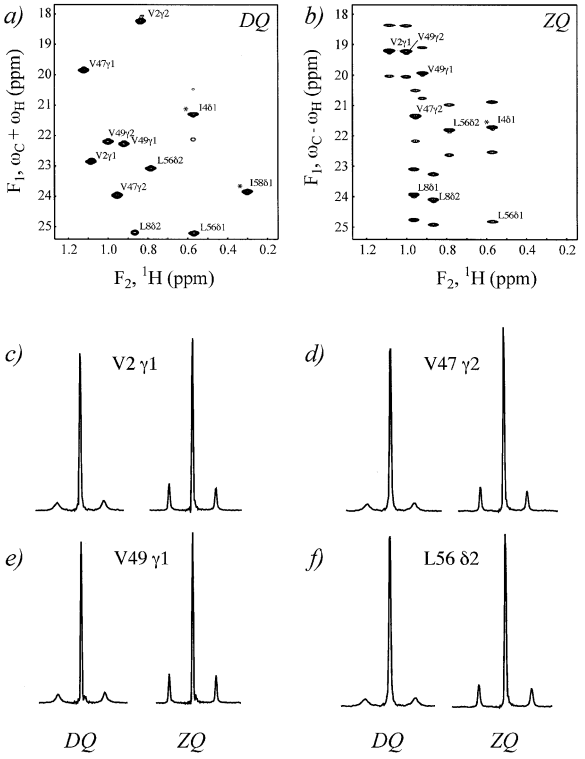

Figure 1. A selected region from ^{1}H-^{13}C DQ (*a*) and ZQ (*b*) spectra recorded on a highly deuterated, U-[^{15}N,^{2}H], Ileδ1-[$^{13}CH_3$], Leu,Val-[$^{13}CH_3/^{12}CD_3$]-labeled sample of protein L, 5 °C (600 MHz). Pulse schemes used are similar to the one illustrated in supplemental material of Tugarinov et al. (2003). The central line of each methyl triplet is labeled with the methyl assignment. Cross-peaks are positioned in F_1 (relative to the ^{13}C carrier) at the sum (DQ) and difference (ZQ) of offsets of ^{1}H and ^{13}C methyl spins from their respective carriers. For simplicity we have labeled the axes exactly as would be done for an HMQC data set. The peaks aliased in F_1 are labeled with asterisks. 1D traces from the F_1 dimensions of DQ and ZQ spectra are shown in (*c*)–(*f*).

not mix these differentially relaxing coherences. That is, slow (fast) relaxing ^{1}H SQ coherences are transformed into slow (fast) relaxing ^{1}H-^{13}C MQ and then subsequently back to slow (fast) decaying ^{1}H magnetization for detection. Moreover, it has further been shown that in ^{1}H,^{13}C DQ or ZQ spectra, a triplet is observed in F_1 and that the outer lines of this triplet are derived from the fast relaxing pathway described above, with the inner line due to the slow relaxing route of coherence transfer (Tugarinov et al., 2003). In applications to high molecular weight proteins the outer triplet components completely disappear and only the central transition, that relaxes in a manner independent of intra-methyl ^{1}H-^{1}H and ^{1}H-^{13}C dipolar fields remains (corresponding to 50% of the signal in the absence of relaxation). This forms the basis of methyl-TROSY spectroscopy that has been described previously (Ollerenshaw et al., 2003; Tugarinov et al., 2003).

Figure 1 shows DQ and ZQ ^{1}H,^{13}C correlation maps recorded on a U-[^{15}N,^{2}H], Ileδ1-[$^{13}CH_3$], Leu,Val-[$^{13}CH_3/^{12}CD_3$]-labeled sample of protein L, using pulse schemes similar to the one described in supplemental material in Tugarinov et al. (2003). Several spectral features are of immediate interest. First, because a small protein is studied here, triplets are observed in F_1 in both DQ and ZQ spectra as described above. Second, the outer lines of triplets derived from the DQ spectrum are less intense than the corresponding outer multiplet components in the ZQ data set. Much smaller differences between the central components of correlations in DQ and ZQ spectra are also observed, due, in large part, to cross-correlated dipolar relaxation interactions between methyl ^{1}H, ^{13}C spins and external ^{1}H and ^{2}H spins; there are no dipolar cross-correlated interactions involving only intra-methyl spins that contribute to the relaxation of the central line (Tugarinov et al., 2003). This effect has been discussed recently and exploited by our group to obtain ZQ methyl-TROSY spectra of high molecular weight proteins that have better resolution than MQ correlation maps (Tugarinov et al., 2004). Here we focus on the outer lines and explore the differences between DQ and ZQ relaxation.

In the absence of spin flips (a very good approximation for highly deuterated, methyl-protonated samples) the difference in relaxation rates between ^{1}H-^{13}C DQ (R_{DQ}) and ZQ (R_{ZQ}) multiplet components is given by $\eta = (R_{DQ} - R_{ZQ})/2$, with

$$\eta = \eta_{HC\text{-}HH} + \eta_{EXT} + \eta_{CSA\text{-}CSA} + \sigma_{CH} + \eta_{EXCH}. \quad (1)$$

In Equation 1 $\eta_{HC\text{-}HH}$ is the cross-correlation rate due to interference between ^{1}H-^{13}C and ^{1}H-^{1}H dipolar interactions within the methyl group, η_{EXT} accounts for cross-correlations between ^{13}C-$^{1}H_{ext}$ and ^{1}H-$^{1}H_{ext}$ as well as ^{13}C-$^{2}H_{ext}$ and ^{1}H-$^{2}H_{ext}$ dipolar interactions, where subscript '*ext*' denotes external spins (i.e., all spins outside the methyl in question), $\eta_{CSA\text{-}CSA}$ is the contribution from ^{13}C CSA – ^{1}H CSA cross-correlation, σ_{CH} accounts for ^{1}H-^{13}C cross-relaxation and η_{EXCH} takes into account (possible) contributions from cross-correlated chemical exchange processes (Konrat and Sterk, 1993; Norwood et al., 1999). The last four terms of Equation 1 are identical for the central and outer components of the methyl triplet. In the macromolecular limit and for an infinitely fast rotating

methyl group, the first term in Equation 1 is given by

$$\eta^{outer}_{HC\text{-}HH} = \frac{3}{5}\frac{\hbar^2\gamma_H^3\gamma_C}{r_{HC}^3 r_{HH}^3}(1 - 3\cos^2\theta_{axis,H-C})S^2_{axis}\tau_c \quad (2)$$

for the outer components, where S_{axis} is an order parameter describing the amplitude of motions of the bond connecting the methyl and its directly attached carbon, τ_c is the correlation time for overall tumbling (assumed isotropic), r_{HC} and r_{HH} are distances between *H-C* and *H-H* atoms in the methyl group and $\theta_{axis,H\text{-}C}$ is the angle between the axis of the methyl group and the *H-C* bond. We have shown previously that in the same limit that Equation 2 applies, $\eta_{HC\text{-}HH} = 0$ for the central line of the triplet (Tugarinov et al., 2003). Therefore the difference between η^{outer} and $\eta^{central}$ provides a measure of the intra-methyl *H-C/H-H* cross correlation rate, Equation 2. Proton spin flips can *decrease* η^{outer} and *increase* $\eta^{central}$ due to cross-relaxation between the outer and central components, artificially decreasing the measured *H-C/H-H* cross correlation rates. Numerical simulations have shown, however, that for highly deuterated, methyl protonated samples of the sort used here, where effective distances to external protons are typically above 3.0 Å, such contributions are small ($< 0.2\ s^{-1}$ for $\tau_c = 10$ ns) and can be safely neglected.

In order to quantify η^{outer} and $\eta^{central}$, a pair of pulse schemes have been developed, Figure 2. The sequence for measuring η^{outer}, Figure 2a, is similar in some respects to an experiment proposed by Tessari and Vuister (2000) for the measurement of DQ/ZQ differential relaxation in ^{1}H-^{15}N two-spin systems. The present case, is however, somewhat more challenging since the spin system considered is more complex. In what follows a brief description of the essential elements of the sequence is provided. At point *a* in the scheme of Figure 2a the coherence of interest is given by the product operator I_XC_Y (sum of DQ and ZQ terms), where A_j is the j-component (j ={x,y,z}) of A magnetization. The subsequent element, of duration $2\zeta = 1/(4J_{HC})$, where J_{HC} is the one-bond ^{1}H-^{13}C scalar coupling constant, leads to purging of the central component; in what follows the only coherences of interest (i.e., that contribute to the detected signal) are those associated with the outer lines of the triplet. This can be seen by noting that immediately prior to the ^{13}C $90_{\phi 2}$ pulse, I_XC_Y has evolved to Σ { $I^i_XC_X$ $(|\alpha\alpha><\alpha\alpha|)^{j,k} - I^i_XC_Y$ $(|\alpha\beta><\alpha\beta| + |\beta\alpha><\beta\alpha|)^{j,k} - I^i_XC_X$ $(|\beta\beta><\beta\beta|)^{j,k}$ }, where α,β are methyl proton spin states and the terms that correspond to the two outer lines ($|\alpha\alpha><\alpha\alpha|$,$|\beta\beta><\beta\beta|$) and the central line ($|\alpha\beta><\alpha\beta| + |\beta\alpha><\beta\alpha|$) have been written explicitly. In the summation the superscripts i,j,k (i≠j≠k) distinguish the three methyl protons, and the sum is over all i. Subsequent application of the $90_{\phi 2}$ pulse (and concomitant phase cycle) eliminates the central line. During the following delay, of duration T, $I^i_XC_X$ evolves due to J_{HC} and relaxation, with the effects of chemical shift refocused. Note that cross-correlated relaxation effects involving ^{1}H-^{13}C dipolar and either of ^{1}H or ^{13}C CSA interactions are also refocused by the π pulse pair in the center of the T period. The choice of ϕ3 = x,ϕ4 = y selects terms of the form $I^i_XC_Y$ that are created during this interval. After ^{13}C chemical shift evolution during t_1, magnetization is transferred back to ^{1}H for detection, leading to cross-peaks at (ω_C,ω_H) with intensity of $C|\sin(2\pi J_{HC}T)\exp(-R_{avg}T)\cosh(\eta^{outer}T)|$, $R_{avg} = (R_{DQ} + R_{ZQ})/2$, where R_{DQ}, R_{ZQ} are the ^{1}H-^{13}C double- and zero-quantum transverse relaxation rates, respectively, and C is a constant. A second data set (ϕ3 = y,ϕ4 = x) is recorded in a manner interleaved with the first (ϕ3 = x,ϕ4 = y), selecting for $I^i_YC_X$ at the end of the T period, and ultimately giving rise to cross-peaks with intensity $C|\sin(2\pi J_{HC}T)\exp(-R_{avg}T)\sinh(\eta^{outer}T)|$. Of note, values of $T = (2k+1)/(4J_{HC})$, k=0,1,2.., are chosen to optimize the sensitivity of the correlations in each of the two data sets. The value of η^{outer} can be extracted from the intensity ratios of the corresponding cross-peaks in each of the two data sets, $|\tanh(\eta^{outer}T)|$, $\eta^{outer} >> 1$, as illustrated below.

Figure 2b shows the pulse sequence that has been developed for measuring $\eta^{central}$. In principle, an experiment similar to the one described above could also be used here, but in practice this would be inefficient since $R_{avg,central} > \eta^{central}$ (on average, by a factor of 4–6; in contrast, $R_{avg,outer} \sim \eta^{outer}$). At point *a* in the pulse scheme, and for ϕ1 = −y, ϕ2 = x, (data set **A**) the coherence of interest is I_YC_Y. The purge element that follows (ϕ3 = y) selects for the central triplet component, so that at the start of the T period a term of the form $\Sigma\{I^i_YC_Y$ $(|\alpha\beta><\alpha\beta|+|\beta\alpha><\beta\alpha|)^{j,k}\}$ is present, referred to in what follows as I_YC_Y for brevity. We note that I_YC_Y is an equal superposition of DQ/ZQ coherences and we focus on the ZQ part for the moment, $1/2(I_YC_Y + I_XC_X)$. The ZQ central component decays exponentially during T, but does not evolve under J_{HC}. After the t_1 period and subsequent transfer of magnetization back to ^{1}H, the magnetiza-

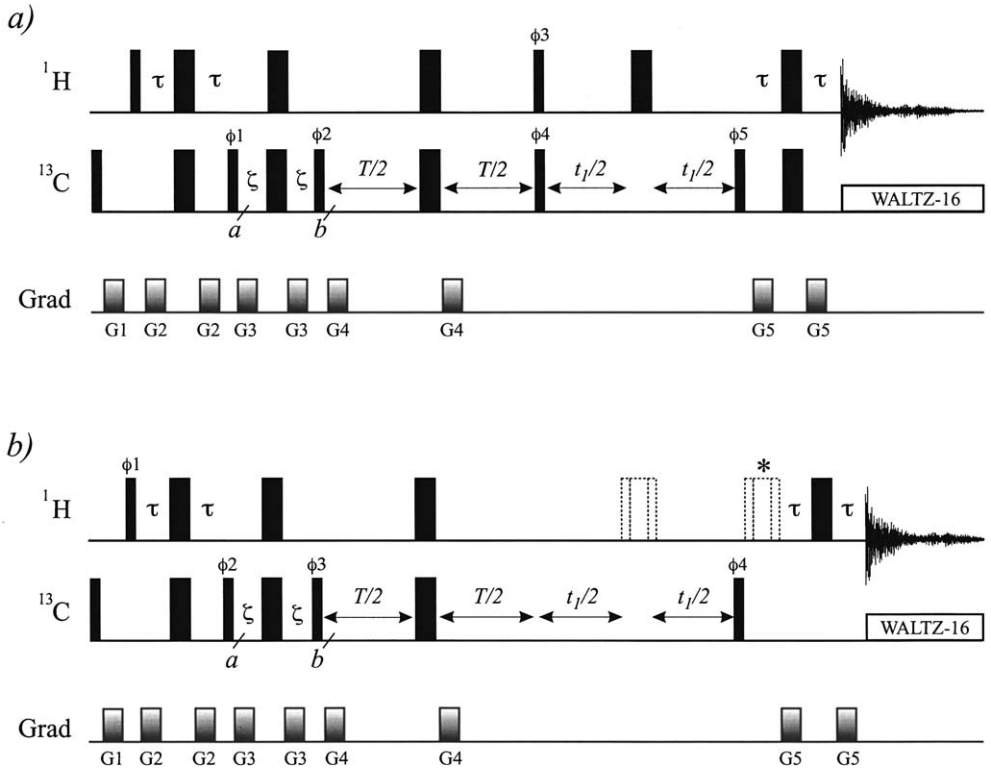

Figure 2. Pulse sequences for the measurement of η^{outer} (*a*) and $\eta^{central}$ (*b*), as described in the text. All narrow (wide) rectangular pulses are applied with flip angles of 90° (180°) along the *x*-axis unless indicated otherwise. The ^{1}H and ^{13}C carriers are positioned in the center of the methyl region: 0.7–1.0 ppm and 18.5–19.0 ppm, respectively. All ^{1}H and ^{13}C pulses are applied with the highest available power, with ^{13}C WALTZ-16 decoupling (Shaka et al., 1983) achieved using a 2 kHz field. The ^{1}H pulses shown with dashed lines are of the composite variety 90°*x*-180°*y*-90°*x* (Levitt and Freeman, 1978). Delays: $\tau = 1.8$ ms, $\zeta = 1.0$ ms $(1/(8^1J_{HC}))$, $T = (2k+1)/(4^1J_{HC})$, k = 0,1,2,... in the case of scheme (*a*). The durations and strengths of the pulsed field gradients applied along the *z*-axis are: G1 = (1.0 ms, 7.5 G/cm), G2 = (0.5 ms, 10 G/cm), G3 = (0.3 ms, −5 G/cm), G4 = (0.4 ms, 12 G/cm), G5 = (0.3 ms, 4.5 G/cm). (*a*) The phase cycle employed is: $\phi 1 = x,-x$; $\phi 2 = 2(x),2(-x)$; $\phi 3 = 8(x),8(-x)$; $\phi 4 = 4(y),4(-y)$; $\phi 5 = x$; rec = $x,-x$. Quadrature detection in F_1 is achieved with States-TPPI incrementation of $\phi 5$ (Marion et al., 1989). Two separate 2D spectra (**A** and **B**) are collected, with phases $\phi 3, \phi 4$ and $\phi 5$ and the phase of the receiver incremented by 90° in **B**. The ratio of correlations in the two spectra is used to obtain η^{outer} (see text); (*b*) The phase cycling employed is: $\phi 1 = -y$; $\phi 2 = 2(x),2(-x)$; $\phi 3 = y,-y$; $\phi 4 = x$; rec = 2(x),2(−x). Two separate 2D data matrices (**A** and **B**, see text) are collected with $\phi 1$, $\phi 3$ incremented by 270° and $\phi 2$ by 90° in data set **B**. Subsequent addition and subtraction of these data sets generates spectra with correlations at single-quantum ^{13}C frequencies decaying with ZQ or DQ rates, respectively. Quadrature detection in F_1 is achieved by recording two separate scans for each t_1 point – with and without the ^{1}H composite 180° pulse marked with an asterisk. For each t_1 increment the phase $\phi 4$ and the receiver phase are incremented by 180°. The resultant data sets are manipulated as described previously for enhanced sensitivity matrices (Cavanagh and Rance, 1993; Kay et al., 1992b).

tion immediately prior to acquisition is $-I^i_X\cos(\omega_C t_1) + I^i_Y\sin(\omega_C t_1)$ in the case that the ^{1}H refocusing pulse indicated by * is not applied. For each value of t_1 a second scan is recorded with this refocusing pulse included (signal immediately prior to acquisition of $I^i_X\cos(\omega_C t_1) + I^i_Y\sin(\omega_C t_1)$) and stored in a separate memory location. Addition and subtraction of the two signals following the enhanced sensitivity F_1-quadrature protocol (Cavanagh and Rance, 1993; Kay et al., 1992b) and subsequent Fourier-transformation gives a cross-peak at (ω_C,ω_H) with intensity proportional to $\exp(-R_{ZQ,central}T)$. A second pathway associated with DQ coherence at point *b* also is present, giving rise to a correlation at $(-\omega_C,\omega_H)$ with intensity proportional to $\exp(-R_{DQ,central}T)$. Double- and zero-quantum signals can be separated by recording an additional data set (interleaved with the first, with and without ^{1}H pulse *, as before) with $\phi 1 = -x,\phi 2 = y,\phi 3 = x$ (data set **B**). In this case the coherence of interest at point *b* is I_XC_X and addition(subtraction) with data set **A** (for which the coherence is I_YC_Y) and subsequent transformation gives rise to ZQ(DQ) spectra (see legend to Figure 1 for details of the phase cycle).

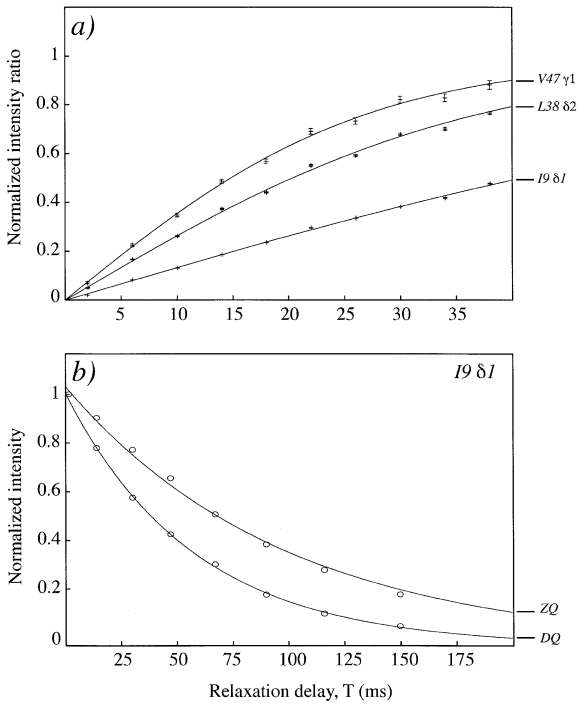

Figure 3. (*a*) Intensity ratios of selected cross-peaks (residues V47γ1, L38δ2 and I9δ1 following a $\tanh(\eta^{outer}T)$ profile, from data sets recorded with the sequence of Figure 2a on a highly deuterated, U-[^{15}N,^{2}H], Ileδ1-[$^{13}CH_3$], Leu,Val-[$^{13}CH_3/^{12}CD_3$]-labeled sample of protein L, 5 °C (600 MHz). Errors in normalized peak intensity ratios were estimated from the noise-level of each spectrum and propagated accordingly. (*b*) Monoexponential decays of DQ and ZQ coherences measured from the central triplet component of the Ile 9 δ1 correlation using the pulse scheme of Figure 2b. Errors in peak intensities lie within the circles denoting experimental points.

A series of such data sets are recorded as a function of T, from which $R_{ZQ,central}$ and $R_{DQ,central}$ are extracted.

Figure 3a shows the $\tanh(\eta^{outer}T)$ build-up of intensity ratios of selected cross-peaks (V47γ1, L38δ2 and I9δ1) obtained using data sets recorded with the sequence of Figure 2a. The decay curves of ZQ and DQ coherences associated with I9δ1 (sequence of Figure 2b) are illustrated in Figure 3b from which $\eta^{central} = (R_{DQ,central}\text{-}R_{ZQ,central})/2$ is obtained. As discussed above in connection with Eq. 1 the difference $\eta^{outer} - \eta^{central}$ eliminates contributions due to *(i)* cross-correlations involving external ^{1}H and ^{2}H spins, *(ii)* ^{1}H-^{13}C cross-relaxation *(iii)* ^{13}C CSA-^{1}H CSA cross-correlations and *(iv)* chemical exchange processes. Thus, $\eta^{outer} - \eta^{central} = \eta^{outer}_{HC\text{-}HH}$, with $\eta^{outer}_{HC\text{-}HH}$ given by Eq. 2. Values of $\eta^{outer}_{HC\text{-}HH}$ for Ile (δ1 only), Leu and Val methyl groups in protein L at a number of different temperatures are listed in Table 1.

Table 1. Experimental η^{outer}-$\eta^{central}$ (s^{-1}) for Ile δ1, Val and Leu methyls of protein L at 5 °C, 15 °C, 25 °C (600 MHz)[a]

Methyl assignment	5 °C	15 °C	25 °C
V2γ1	51.9 ± 0.8	36.0 ± 0.2	24.7 ± 0.6
V2γ2	49.2 ± 0.5	32.2 ± 0.2	22.6 ± 0.5
I4δ1	26.1 ± 0.1	17.7 ± 0.1	12.0 ± 0.1
L8δ1	12.1 ± 0.1	8.4 ± 0.1	5.9 ± 0.1
L8δ2	13.1 ± 0.1	9.1 ± 0.1	6.7 ± 0.1
I9δ1	28.4 ± 0.1	19.9 ± 0.1	13.7 ± 0.1
L38δ1	38.0 ± 0.6	25.8 ± 0.1	17.8 ± 0.2
L38δ2	35.6 ± 0.4	23.4 ± 0.1	16.2 ± 0.2
V47γ1	47.9 ± 1.0	30.3 ± 0.2	20.5 ± 0.6
V47γ2	52.4 ± 0.5	34.5 ± 0.2	23.3 ± 0.6
V49γ1	51.9 ± 1.2	36.0 ± 0.2	23.7 ± 0.6
V49γ2	45.9 ± 0.7	31.2 ± 0.2	21.3 ± 0.5
L56δ1	44.7 ± 1.1	29.8 ± 0.1	20.3 ± 0.4
L56δ2	43.0 ± 0.3	29.3 ± 0.1	20.2 ± 0.4
I58δ1	42.3 ± 0.1	29.1 ± 0.1	20.2 ± 0.2

[a]Errors were estimated separately for η^{outer} and $\eta^{central}$ rates from 200 Monte-Carlo simulations using uncertainties in peak intensities and subsequently propagated to the difference η^{outer}-$\eta^{central}$.

The implication of Eq. 2 above is that $\eta^{outer}_{HC\text{-}HH}$ values can be used to provide estimates of side chain flexibility so long as the overall tumbling of the molecule is slow, methyl three-fold rotation is fast and the methyl geometry is known accurately. We have assumed a value of -0.228 Å^{-3} for $P_2(\cos\theta_{axis,H\text{-}C})/r^3_{HC}$ obtained from dipolar coupling based studies (Mittermaier and Kay, 2002; Ottiger and Bax, 1999). A value of $r_{HC} = 1.117$ Å proposed by Ottiger and Bax (1999) corresponds to $\theta_{axis,H\text{-}C} = 110.4°$ from which the distance r_{HH} can be calculated from the geometry of the methyl group as $r_{HH} = \sqrt{3} r_{HC} \sin(\theta_{axis,H\text{-}C})$. Figure 4 shows quantitative correlations between methyl axis order parameters calculated from intra-methyl *H-C/H-H* dipolar cross-correlation rates discussed here ($\eta^{outer}_{HC\text{-}HH}$) and those obtained from ^{2}H relaxation data (Skrynnikov et al., 2002) over a temperature range extending from 5–25 °C. Correlation coefficients between the two sets of order parameters are greater than 0.98 despite the fact that contributions from local motions are neglected in Eq. 2.

The agreement between order parameters derived from $\eta^{outer}_{HC\text{-}HH}$ and from ^{2}H spin relaxation measurements does decrease significantly for molecular tumbling times less than about 5 ns (25 °C). Notably the correlation is still very good with correlation

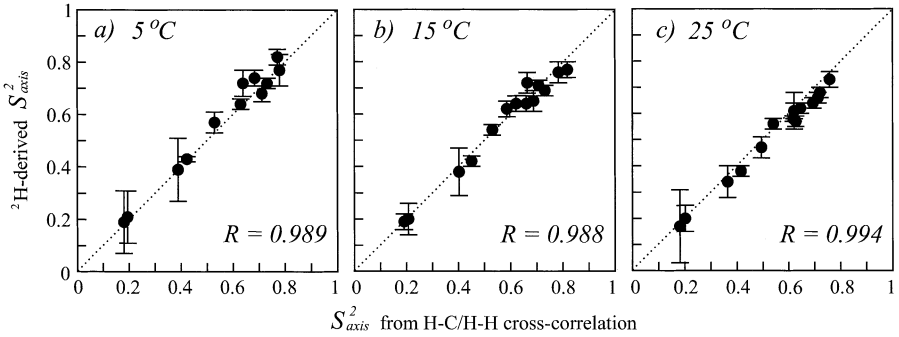

Figure 4. Correlations between methyl axes order parameters derived from (*i*) ^{2}H spin relaxation measurements on a fractionally deuterated, ^{13}C labeled protein L sample (Skrynnikov et al., 2002), Y-axis, and (*ii*) those measured in this work from *HC/HH* dipolar cross-correlated relaxation using Eq. 2, X-axis. Correlations at 5 °C (τ_c, correlation time in D_2O = 10.2 ns) (*a*), 15 °C (τ_c = 6.7 ns) (*b*) and 25 °C (τ_c = 5.0 ns) (*c*) are shown. Correlation coefficients are indicated in the right bottom corner of the plots. ^{2}H relaxation data for Ile 4 δ1, Leu 8 δ1 and δ2 could only be properly fit with a model which includes ns time-scale dynamics (LS-3 model, in which a correlation time, $\tau_{c,eff}$, smaller than τ_c is assumed, Skrynnikov et al. (2002)). For these residues $\tau_{c,eff}$ has been used in place of τ_c in Equation 2. Errors in ^{2}H derived order parameters are indicated with vertical bars; the three residues for which the largest errors in order parameters were obtained are those whose relaxation data could only be fit with the more complex LS-3 model in which there is some interplay between $\tau_{c,eff}$ and S^2 (and hence the larger errors). Random errors derived from the cross-correlation measurements are less than the size of the data points, however, systematic errors due to uncertainties in methyl geometry are very likely substantially larger.

coefficients greater than 0.96. However, the cross-correlation derived order parameters become significantly larger than values obtained from ^{2}H data (∼25–30% for protein L at 45 °C, τ_c = 2.1 ns), to the point where they actually increase with temperature (S^2 values from cross-correlation are on average 17% higher at 45 °C than at 5 °C). As the overall correlation time decreases it is clear that the assumptions associated with Eq. 2 break down and spectral densities evaluated at higher frequencies must be taken into account, along with contributions from methyl rotation. Simulations show that providing the timescale of methyl rotation is known and that all spectral densities of relevance are included, it should be possible to extract accurate order parameters even outside the macromolecular tumbling limit. However, we have not succeeded in improving the agreement between ^{2}H and ^{13}C/^{1}H cross-correlation derived order parameters for τ_c < ∼5 ns at this point. Of interest, order parameters that are too large have also been obtained from other ^{13}C-based relaxation measurements developed in our laboratory when such experiments are performed on proteins with small correlation times (∼5 ns or less). We are in the process of investigating this further. ^{2}H spin relaxation studies (Muhandiram et al., 1995), with the inherent consistency-check associated with the measurement of 5 available rates (Millet et al., 2002; Skrynnikov et al., 2002), remain the approach of choice for obtaining accurate measures of side chain dynamics.

In summary, we have shown that there are significant differences in the relaxation rates of multiplet components that contribute to observed signals in ^{1}H-^{13}C multiple-quantum spectroscopy. The dominant contributor to the differences in relaxation of outer multiplet components of correlations in DQ and ZQ spectra derives from intra-methyl *H-C/H-H* dipole cross-correlation. In applications to large proteins (for example, malate synthase G, 82 kDa (Tugarinov et al., 2002)) these outer components are not observed (except for 1 or 2 very flexible residues) in either DQ or ZQ spectra (Tugarinov et al., 2003). However, in small proteins the outer multiplets can be observed and differences in relaxation quantified. New NMR experiments are presented for the measurement of this cross-correlation effect in such systems. Measured *H-C/H-H* cross-correlation rates are shown to be sensitive probes of side chain order. Moreover, studies of protein L here suggest that accurate order parameters derived from intra-methyl *H-C/H-H* cross-correlation can be obtained in applications involving proteins with correlation times in excess of approximately 5 ns, providing that the outer multiplet components can be observed in the first place.

Acknowledgements

This work was supported by a grant from the Canadian Institutes of Health Research (CIHR) to L.E.K. We thank Dr Voula Kanelis (University of Toronto) for providing the sample of protein L and Dr Oscar Millet (University of Toronto) for sharing with us the results of ^{2}H relaxation measurements. V.T. acknowledges the support of the Human Frontiers Science Program. L.E.K. holds a Canada Research Chair in Biochemistry.

References

Cavanagh, J. and Rance, M. (1993) *Annu. Rep. NMR Spectrosc.*, **27**, 1–58.

Cho, C.H., Urquidi, J., Singh, S. and Robinson, G.W. (1999) *J. Phys. Chem. B.*, **103**, 1991–1994.

Delaglio, F., Grzesiek, S., Vuister, G.W., Zhu, G., Pfeifer, J. and Bax, A. (1995) *J. Biomol. NMR*, **6**, 277–293.

Gardner, K.H. and Kay, L.E. (1997) *J. Am. Chem. Soc.*, **119**, 7599–7600.

Goto, N.K., Gardner, K.H., Mueller, G.A., Willis, R.C. and Kay, L.E. (1999) *J. Biomol. NMR*, **13**, 369–374.

Kay, L.E. and Bull, T.E. (1992) *J. Magn. Reson.*, **99**, 615–622.

Kay, L.E. and Prestegard, J.H. (1987) *J. Am. Chem. Soc.*, **109**, 3829–3835.

Kay, L.E. and Torchia, D.A. (1991) *J. Magn. Reson.*, **95**, 536–547.

Kay, L.E., Bull, T.E., Nicholson, L.K., Griesinger, C., Schwalbe, H., Bax, A. and Torchia, D.A. (1992a) *J. Magn. Reson.*, **100**, 538–558.

Kay, L.E., Keifer, P. and Saarinen, T. (1992b) *J. Am. Chem. Soc.*, **114**, 10663–10665.

Konrat, R. and Sterk, H. (1993) *Chem. Phys. Lett.*, **203**, 75–80.

Levitt, M. and Freeman, R. (1978) *J. Magn. Reson.*, **33**, 473–476.

Marion, D., Ikura, M., Tschudin, R. and Bax, A. (1989) *J. Magn. Reson.*, **85**, 393–399.

Millet, O., Muhandiram, D.R., Skrynnikov, N.R. and Kay, L.E. (2002) *J. Am. Chem. Soc.*, **124**, 6439–6448.

Mittermaier, A. and Kay, L.E. (2001) *J. Am. Chem. Soc.*, **123**, 6892–6903.

Mittermaier, A. and Kay, L.E. (2002) *J. Biomol. NMR*, **23**, 35–45.

Muhandiram, D.R., Yamazaki, T., Sykes, B.D. and Kay, L.E. (1995) *J. Am. Chem. Soc.*, **117**, 11536–11544.

Muller, N., Bodenhausen, G. and Ernst, R.R. (1987) *J. Magn. Reson.*, **75**, 297–334.

Norwood, T.J., Tillett, M.L. and Lian, L.Y. (1999) *Chem. Phys. Lett.*, **300**, 429–434.

Ollerenshaw, J.E., Tugarinov, V. and Kay, L.E. (2003) *Magn. Reson. Chem.*, **41**, 843–852.

Ottiger, M. and Bax, A. (1999) *J. Am. Chem. Soc.*, **121**, 4690–4695.

Palmer, A.G., Wright, P.E. and Rance, M. (1991) *Chem. Phys. Lett.*, **185**, 41–46.

Prestegard, J.H. and Grant, D.M. (1978) *J. Am. Chem. Soc.*, **100**, 4664–4668.

Scalley, M.L., Yi, Q., Gu, H., McCormack, A., Yates, J.R. and Baker, D. (1997) *Biochemistry*, **36**, 3373–3382.

Shaka, A.J., Keeler, J., Frenkiel, T. and Freeman, R. (1983) *J. Magn. Reson.*, **52**, 335–338.

Skrynnikov, N.R., Millet, O. and Kay, L.E. (2002) *J. Am. Chem. Soc.*, **124**, 6449–6460.

Tessari, M. and Vuister, G.W. (2000) *J. Biomol. NMR*, **16**, 171–174.

Tugarinov, V. and Kay, L.E. (2004) *J. Biomol. NMR*, **28**, 165–172.

Tugarinov, V., Hwang, P., Ollerenshaw, J. and Kay, L.E. (2003) *J. Am. Chem. Soc.*, **125**, 10420–10428.

Tugarinov, V., Muhandiram, R., Ayed, A. and Kay, L.E. (2002) *J. Am. Chem. Soc.*, **124**, 10025–10035.

Tugarinov, V., Sprangers, R. and Kay, L.E. (2004) *J. Am. Chem. Soc.*, **126**, 4921–4925.

Vold, R.L. and Vold, R.R. (1978) *Prog. NMR Spectrosc.*, **12**, 79–133.

Vold, R.R. and Vold, R.L. (1976) *J. Chem. Phys.*, **64**, 320–332.

Werbelow, L.G. and Grant, D.M. (1977) *Adv. Magn. Reson.*, **9**, 189–299.

Werbelow, L.G. and Marshall, A.G. (1973) *J. Magn. Reson.*, **11**, 299–313.